Available online at www.sciencedirect.com
SCIENCE DIRECT®
Polymer 44 (2003) 4881–4887
polymer
www.elsevier.com/locate/polymer

Characterization of hyperporous polyurethane-based gels by non-intrusive mercury porosimetry

R. Pirard[a,*], A. Rigacci[b], J.C. Maréchal[c], D. Quenard[c], B. Chevalier[c], P. Achard[b], J.P. Pirard[a]

[a]*Laboratoire de Génie Chimique, Institut de Chimie B6a, Université de Liège, B-4000 Liège, Belgium*
[b]*Ecole des Mines de Paris, CENERG, BP 207, F-06904 Sophia-Antipolis Cedex, France*
[c]*Centre Scientifique et Technique du Bâtiment, 24 rue Joseph Fourier, F-38402 Saint-Martin d'Hères, France*

Received 26 September 2002; received in revised form 22 April 2003; accepted 30 May 2003

Abstract

Evaporative drying of polyurethane-based gels produces xerogels. Supercritical drying after replacement of interstitial liquid by supercritical CO_2 produces aerogels. SEM micrographs show that both materials are made up of small size particles gathered up in filament-shaped, strongly cross-linked aggregates. Density measurements show that they both have a large pore volume.

When submitted to mercury porosimetry, the behavior of these materials is similar to that of inorganic aerogels, as previously observed. Mercury does not penetrate the pore network, but the whole material is densified. The usual Washburn equation cannot be used to analyze the mercury porosimetry. A well-suited equation based on a buckling model of filament-shaped aggregates has been developed in order to determine the pore volume distribution of mineral dried gels. This equation is also valid for analyzing the texture of organic hyperporous materials like polyurethane dried nanoporous gel.

Keywords: Dried gels; Porous texture; Mercury porosimetry

1. Introduction

Mercury porosimetry is a method currently used to characterize the texture of porous materials. It allows determining the pore volume, specific surface area and distributions of pore volume and surface area versus the pore size. The generally accepted basic hypothesis is that mercury penetrates into narrower and narrower cavities, or pores, as pressure increases. Data analysis is performed using the intrusion equation proposed by Washburn [1]

$$r = \frac{2\gamma \cos\theta}{P} \quad (1)$$

in which r is the cylindrical pore radius, P, the pressure at which mercury penetrates into the pore, γ, the surface tension of mercury (0.485 N/m) and θ, the contact angle between the mercury meniscus and a flat non-metallic surface ($\theta \approx 140°$).

In early applications of the method it appeared that porous or non-porous materials were elastically compressed at high pressures. To obtain accurate results, the volume variation due to compression must be subtracted from the rough data. In the case of porous materials, however, volume variation due to elastic compression is often negligible compared to the volume variation due to mercury intrusion into the empty pores. Mercury porosimetry data are thus generally handled without any correction.

Using mercury porosimetry to characterize monolithic materials with a very large pore volume, like silica aerogels, some authors have observed that mercury does not penetrate into the pores, but pressure causes densification of the material [2]. Inorganic aerogels are synthesized by the sol–gel process, which consists in hydrolysis and condensation of mineral alkoxides in an alcoholic solvent, leading to a nanostructured gel. After gelation and aging, the material is usually dried at a temperature and pressure higher than the critical point of the interstitial solvent. Supercritical drying prevents the tenuous material from shrinking because of solvent surface tension forces. Consequently, supercritical drying, while preserving the material texture, leads to very porous materials [3]. When a monolithic sample of an aerogel is submitted to mercury porosimetry, it is easy to

* Corresponding author. Tel.: +32-43664758; fax: +32-43663545.
E-mail address: r.pirard@ulg.ac.be (R. Pirard).

0032-3861/03/$ - see front matter © 2003 Elsevier Science Ltd. All rights reserved.
doi:10.1016/S0032-3861(03)00481-6

recover and examine the sample after the experiment and to see that its overall volume has strongly decreased and that no traces of mercury are entrapped in the pore network. The mechanism of volume variation is thus not the intrusion of mercury in the pores, so Washburn's equation cannot be applied for analysis. If used, this equation leads to pore sizes that are overestimated by several orders of magnitudes, as shown by comparison with SEM observation.

In a previous publication [4], the pore size distribution of an aerogel previously densified under different mercury isostatic pressures was measured by the nitrogen sorption method. It was established that during densification, mercury isostatic pressure entirely crushes pores whose size exceeds a limit size L, which is a function of the pressure P. Pores smaller than the limit size remain unaffected. The relation between L and P has been determined as

$$L = \frac{k_f}{P^{0.25}} \tag{2}$$

The mechanism of pore collapse has been identified with the buckling of filament-shaped mineral oxide aggregates under an axial compressive stress. The critical stress for buckling can be obtained from Euler's law. Consequently, the value of the k_f constant depends on: Young's modulus of filament-shaped aggregates made of microporous particles, on the diameter of these filaments and on their arrangement in space. These three values cannot be easily determined individually, and until now, the k_f constant had to be experimentally determined for each material. The determination of k_f can be made by measuring the size L of the largest pores remaining after compression at a pressure P. For this purpose, pore size is usually obtained by analysis of nitrogen adsorption-desorption isotherms. The knowledge of k_f allows computing pore volume distribution versus pore size, using Eq. (2).

More recently it has been observed that the densification of porous materials under isostatic mercury pressure is not restricted to aerogels. In many very porous materials, the mercury isostatic pressure causes collapse of the pores before the pressure is high enough to cause mercury intrusion, at least in a limited pressure domain. This phenomenon is observed on mineral materials synthesized by the sol–gel process, aerogels and porous xerogels [4,5], on highly dispersive silica (HDS) precipitated from alkaline silicate [6], on fumed silica [7] and sometimes on carbon black [8].

In addition to their behavior under mercury isostatic pressure, these materials have several other common characteristics: they have a large pore volume, generally more than 1 cm^3/g, and they are made up of small size particles gathered up in filament-shaped, strongly cross-linked aggregates. Pirard calls them by the generic name, 'hyperporous materials', and has studied them in detail [9].

Most hyperporous materials are densified by mercury pressure only in the low-pressure range. Beyond a pressure P_t, mercury intrusion occurs in small size pores, that remain unaffected by densification at low pressures. This more complex behavior allows one to easily obtain the value of k_f, as shown hereafter. Typical examples of such materials are the hyperporous silica xerogels, which can be synthesized in monolithic shape and whose behavior can easily be described [5,10].

The present paper shows that some organic materials, particularly polyurethane aerogels and xerogels, submitted to mercury porosimetry, have behaviors similar to those of silica xerogels and aerogels. They are made up of particles grouped in chain-like aggregates. These polyurethane-based gels are hyperporous and their pore texture can be studied by mercury porosimetry, using the buckling Eq. (2).

Such nanostructured organic materials may present advantages in the thermal superinsulation field before [11] or after pyrolysis [12]. Indeed, like all types of aerogels [13] their nanoporous structure leads to effective thermal conductivity significantly lower than the conductivity of air (0.026 W/m K at room temperature and atmospheric pressure). Furthermore, in comparison with silica aerogels and xerogels, in their organic state or as carbon materials after pyrolysis, they absorb the infrared contribution of the thermal transport, which may present an advantage at moderate or high temperatures.

2. Experimental

On the basis of sol–gel processing, the synthesis of monolithic polyurethane-based gels has been explored to elaborate, after a suitable drying step, monolithic aerogels and xerogels for further preliminary structural characterization [14]. The sol–gel route used here is based on the polyaddition reactions between polyol and polyisocyanate molecules used as precursors, leading to a polyurethane polymer with a high degree of cross-linking.

The reactives were first dissolved in a suitable organic medium, where both the monomers and the growing polyurethane particles were soluble. After adding the catalyst, gelation occurred at ambient temperature. Cure time varied from 15 min to 2 days, depending on various chemical operating variables, like the catalyst ratio, the nature of the organic media, the nature of the isocyanate (aromatic or aliphatic) and of the polyol (hydroxyl content, primary or secondary hydroxyl), the ratio between polyol and isocyanate and the dilution ratio of the sol. All these combined factors govern the aggregation process and the reaction kinetics, and so the final structure of the gel.

After gelation and aging, the gels were dried in two different ways. On one hand, xerogels (X) were obtained by slowly evaporating the solvent at ambient temperature and atmospheric pressure [3]. On the other hand, aerogels (A) were obtained by extraction of CO_2 in supercritical conditions—around 37 °C, 8 MPa—[15]. Organic solvent, contained in the totally opened porosity of the wet gels, was

directly exchanged with supercritical CO_2 in an autoclave. The CO_2 was finally slowly and isothermally − 10 kPa/min at 37 °C—evacuated from the gels, which led to monolithic and crack-free polyurethane aerogels [16]. One can note that a preliminary organic exchange of solvent was performed before drying in order to facilitate the posterior exchange with supercritical CO_2.

Characterization was performed on dry gels. The bulk density of the polyurethane aerogels and xerogels was classically estimated, thanks to weight and size measurements or by mercury pycnometry, and the true density of the polyurethane skeleton was measured by helium pycnometry (Micromeritics Accupyc 1330). Mercury porosimetry was performed from 0.01 to 200 MPa on samples evacuated during 4 h under 1.3 Pa (Carlo-Erba Porosimeter 2000). The microstructure was also observed by SEM (Jeol JSM840).

3. Results

Four aerogels (A) and two xerogels (X) were investigated in this study. Dried xerogel and aerogel products were monolithic, as shown in Fig. 1. Surprisingly, the bulk density of the xerogels was systematically lower than that of the aerogels (Table 1).

Mercury porosimetry is the most attractive method allowing the determination the pore texture from 7.5 nm to a diameter that depends on the mechanism of volume variation. Three different behaviors were observed on the various samples. Sample S1A accepts the penetration of mercury in the whole pressure range (Fig. 2(a)). Data analysis using Eq. (1) leads to a pore size distribution (Fig. 2(b)) centered on 5500 nm.

Samples S5A and S6A, submitted to mercury porosimetry, show a volume variation when the pressure increases beyond 1 MPa, but no volume variation is observed when the pressure decreases (Fig. 3(a)). The phenomenon is irreversible. Samples were recovered and observed after the experiment, which was possible because they were monolithic. Their mass remained unchanged, showing that no mercury was entrapped in the pores. Their specific volume was measured by mercury pycnometry and was

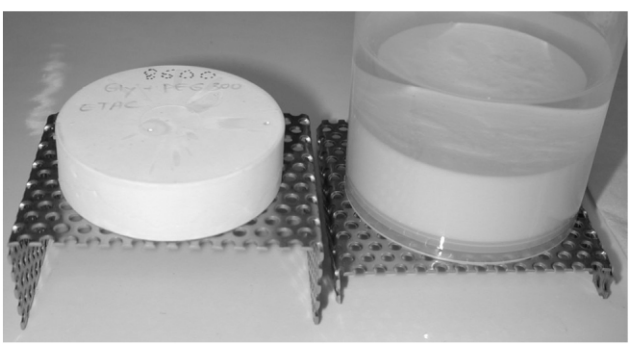

Fig. 1. Hyperporous polyurethane samples before (right) and after (left) direct supercritical CO_2 drying.

Table 1
Sample properties

Sample	ρ_t ($\pm$0.01, g/cm^3)	ρ_b ($\pm$0.03, g/cm^3)	D (μm)	P_t (MPa)	k_f (nm MPa$^{0.25}$)
S1A	1.43	0.26	2	<0.1	>8500
S2X	1.24	0.11	1.4	0.2	5000
S3X	1.21	0.15	1.2	0.6	2200
S4A	1.16	0.27	0.12	10	266
S5A	1.19	0.37	~0.05	>200	<28
S6A	1.23	0.28	~0.05	>200	<28

ρ_t : true density obtained by helium pycnometry. ρ_b : bulk density obtained by monolith weighing and linear measurements. D : particle size estimated by SEM. P_t : pressure of change of mechanism during mercury porosimetry measurement. k_f : buckling strength constant. A: supercritical drying leading to Aerogels. X: evaporative drying at ambient temperature and atmospheric pressure leading to Xerogels.

found to be 0.8 cm^3/g in both cases. This can be compared with the specific volume of the samples S5A and S6A before the experiment, respectively, 2.7 and 3.6 cm^3/g. These results mean that no mercury penetrated the samples during the pressure increase, but that their bulk volume was reduced. The mercury porosimetry data cannot be analyzed using the intrusion Eq. (1). Investigations by SEM showed that these materials are made up of chain-like aggregates of particles. This observation allows considering these samples as hyperporous materials. Consequently their mercury

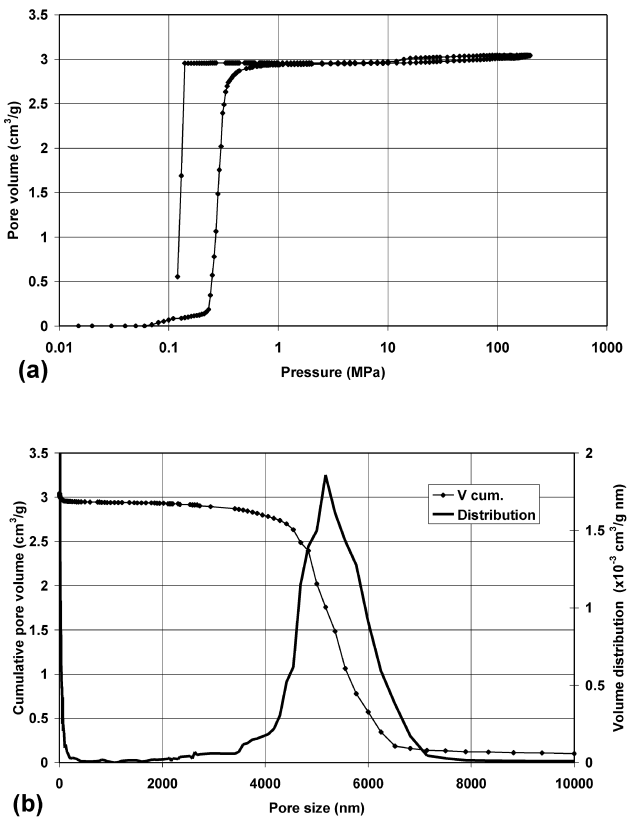

Fig. 2. Textural characterization of sample S1A. (a) Mercury porosimetry raw data, volume versus pressure and (b) Cumulative pore volume and pore volume distribution as a function of pore size.

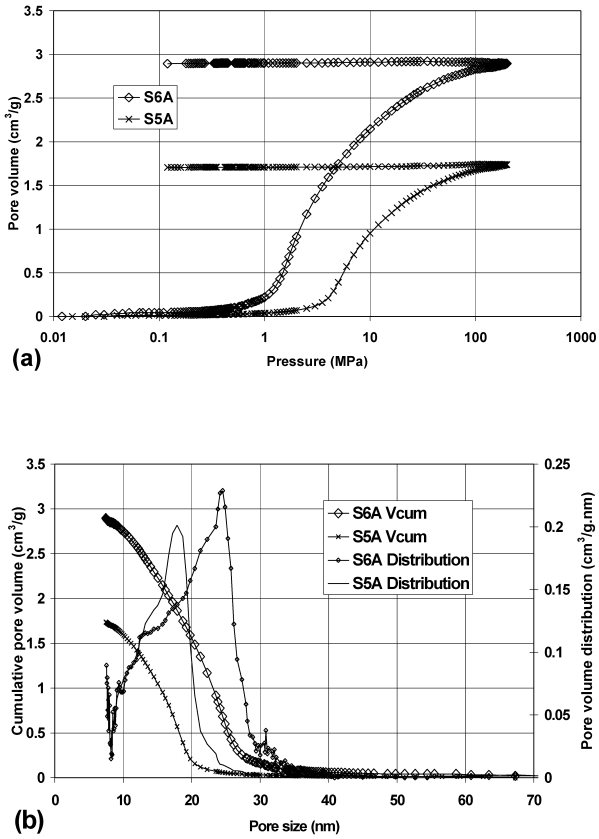

Fig. 3. Textural characterization of samples S5A and S6A. (a) Mercury porosimetry raw data, volume versus pressure and (b) Cumulative pore volume and pore volume distribution as a function of pore size.

porosimetry data must be analyzed by the buckling Eq. (2). The obtained distributions (Fig. 3(b)) show that both samples contain only pores with sizes below 35 nm. The use of the inappropriate Eq. (1) would have led to a wrong distribution with pore size as large as 1500 nm, which is invalidated by SEM observations

Samples S2X, S3X and S4A show a more complicated behavior when submitted to mercury porosimetry (Fig. 4(a)). The increasing pressure branch of the plots volume versus pressure shows that the volume increases roughly proportionally to the logarithm of pressure. However, the proportionality factor suddenly changes when the pressure reaches P_t, estimated at 0.2, 0.58 and 10 MPa for samples S2X, S3X and S4A, respectively. For each sample, the porosimetry experiment was repeated and interrupted just before the pressure reached P_t. The monolithic samples recovered after such partial pressurization were weighed and observed. It was noted that the mass was unchanged and that the volume was reduced. This means that no intrusion occurred, but rather that the samples were just densified. Mercury porosimetry was then carried out beyond P_t until the maximum pressure (200 MPa). Examination on recovered full-pressurized samples showed that some mercury remains entrapped and that samples have gained weight, but the bulk volume is the same as for samples recovered after the experiment at pressure P_t. The behavior of these materials is identical to that of silica xerogels, which means that they are densified without intrusion when the pressure is less than P_t and penetrated by mercury without volume change when the pressure is higher [17]. The data analysis can be made with the buckling Eq. (2) for pressures below P_t and with the classical Washburn Eq. (1) for pressures higher than P_t. At pressure P_t, both equations are simultaneously valid, which allows computing the value of the buckling constant k_f (Table 1) by Eq. (3).

$$k_f = \frac{4\gamma \cos\theta}{P_t^{0.75}} \tag{3}$$

Using the correct equation, pore volume distributions versus pore size can be determined for each sample (Fig. 4(b), (c) and (d)).

SEM observations (Fig. 5(a)–(f)) show that all the polyurethane-based gels are made up of chain-like aggregated particles with large empty spaces, which are pores, found on both sides of the aggregates. Rough evaluation of the size of the largest pores can be estimated and confirms values obtained from mercury porosimetry. Particle size D (Table 1), and consequently the thickness of chain-like aggregates, varies from one sample to another and can also be estimated. Because the thickness (about 20 nm) of the metallization layer essential to allow SEM examination, the size of smallest particles—samples S5A and S6A—can only be evaluated by an order of magnitude. It is also important to note that some samples have simply juxtaposed particles, while others have partially interpenetrated particles.

4. Discussion

Polyurethane gels are synthesized in an organic media by addition reaction of polyisocyanate with polyol. The reaction products are insoluble particles that group together in aggregates. The chain-like aggregates are cross-linked and form a three-dimensional network, which is the solid skeleton of the monolithic gel. The pore sizes of samples S2X and S3X (Fig. 4(b) and (c)) are large enough to induce small capillary stress. The structure of the gel, which is very open as observed by SEM (Fig. 5(b) and (c)), allows an easy elimination of the solvent, even during a simple evaporation drying process. In spite of a partial shrinkage of the gel occurring during evaporative drying, due to the surface tension of the solvent, the pore volume of the dry gel can be considerable, reaching 6 cm^3/g. In case of supercritical drying in carbon dioxide, surface tensions theoretically vanish and no shrinkage occurs. Consequently, gels with smaller mean pore sizes can be supercritically dried without prejudicial densification, as appears for samples S4A, S5A and S6A (Figs. 4(d) and 3(b)).

The materials studied have a structure made up of particles that are aggregated in cross-linked, chain-like aggregates, with a large pore volume. When submitted to

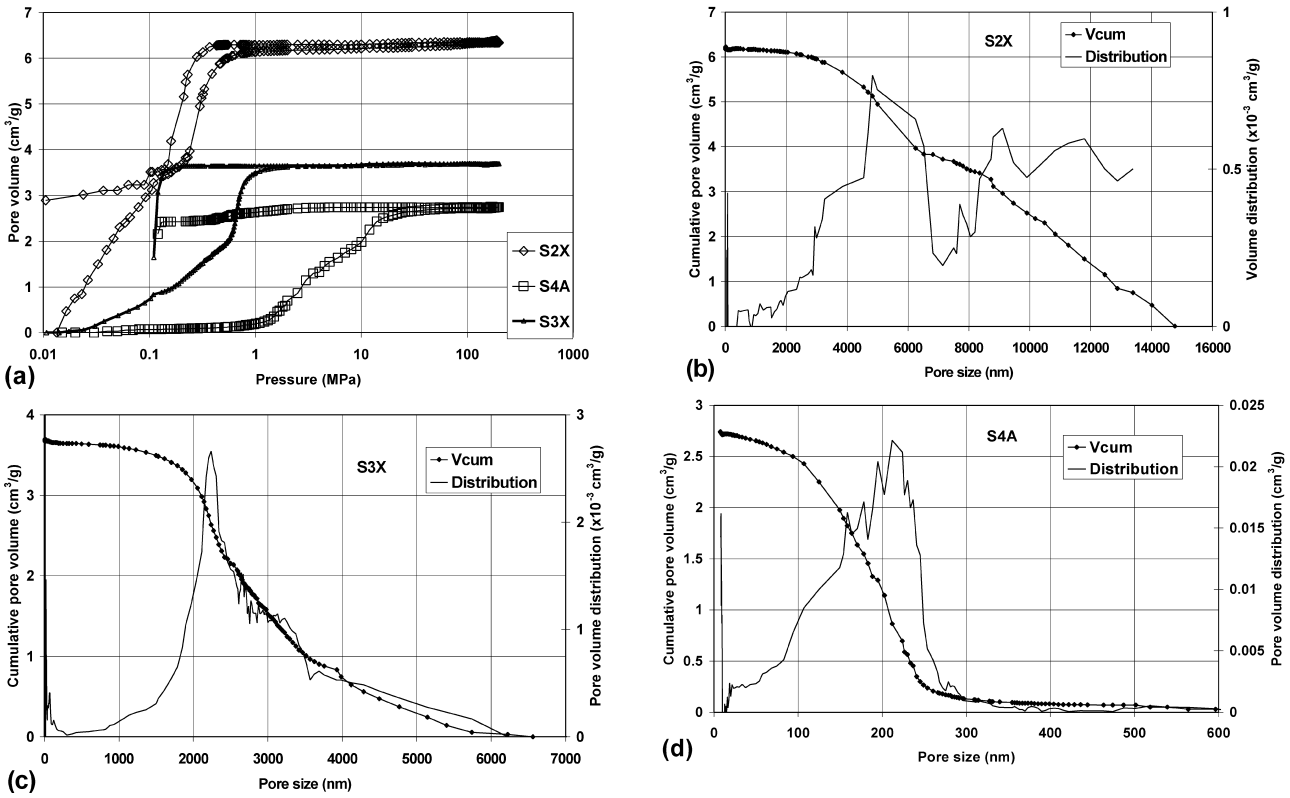

Fig. 4. Textural characterization of samples S2X, S3X and S4A. (a) Mercury porosimetry raw data, volume versus pressure, (b) Cumulative pore volume and pore volume distribution as a function of pore size of sample S2X, (c) Cumulative pore volume and pore volume distribution as a function of pore size of sample S3X and (d) Cumulative pore volume and pore volume distribution as a function of pore size of sample S4A.

mercury porosimetry, and at least in a limited range of pressure, they shrink and are not penetrated by mercury. This category of material is called 'hyperporous' [9]. Mercury pressure applied to the external surface of samples of these materials generates compressive stress in the aggregates that constitute the solid skeleton of the material. If the skeleton is strong enough, it can resist the pressure and the mercury can penetrate into the largest pores when the pressure is high enough. In the case of hyperporous materials, the skeleton is weak. Chain-like aggregates, submitted to an axial stress are bent and the longest aggregates buckle. The largest pores between the longest aggregates collapse at a pressure below the pressure at which the mercury would penetrate a pore of the same size. Eq. (2) expresses the buckling mechanism according to Euler's equation. It relates the pressure P and the length L of chain-like aggregates between two branching points. According to Euler's law, the constant k_f expresses

$$k_f = \frac{d(n^2 \cdot \pi^2 \cdot E)^{0.25}}{2} \quad (4)$$

in which d is the diameter of the chain-like aggregates. The buckling mode is expressed by the integer n and E is the Young modulus of aggregates. For silica xerogels it was shown that a linear relationship exists between k_f, determined experimentally and d measured by TEM [17,18]. On the polyurethane-based gels, the thickness d of aggregates is difficult to estimate, and it is assumed that it is roughly proportional to particle diameter D, which is more easily measured on SEM micrographs. The data (Table 1 and Fig. 6) show an increase of k_f in function of D, compatible with Euler's Eq. (4). It is noted that, as shown in Fig. 5(a) and (b), particles in samples S1A and S2X are partially interpenetrated, unlike sample S3X (Fig. 5(c)), where the particles are only juxtaposed. The buckling strength of the aggregates with interpenetrated particles is higher than that of aggregates with simply juxtaposed particles. Consequently, the linear relationship is only rough.

5. Conclusions

The polyurethane gels investigated in this study are made of particles aggregated in cross-linked chain-like aggregates with large pores between them. The particle size distribution is very narrow and the mean size varies with the nature and concentration of the polyol and with the drying route used. The samples submitted to mercury porosimetry show an unusual behavior; in a large pressure range, the recorded volume variation corresponds to a bulk volume reduction of the sample, and not to an intrusion of mercury into the pore network. This behavior combined with a large pore volume and with the typical microstructure of materials in

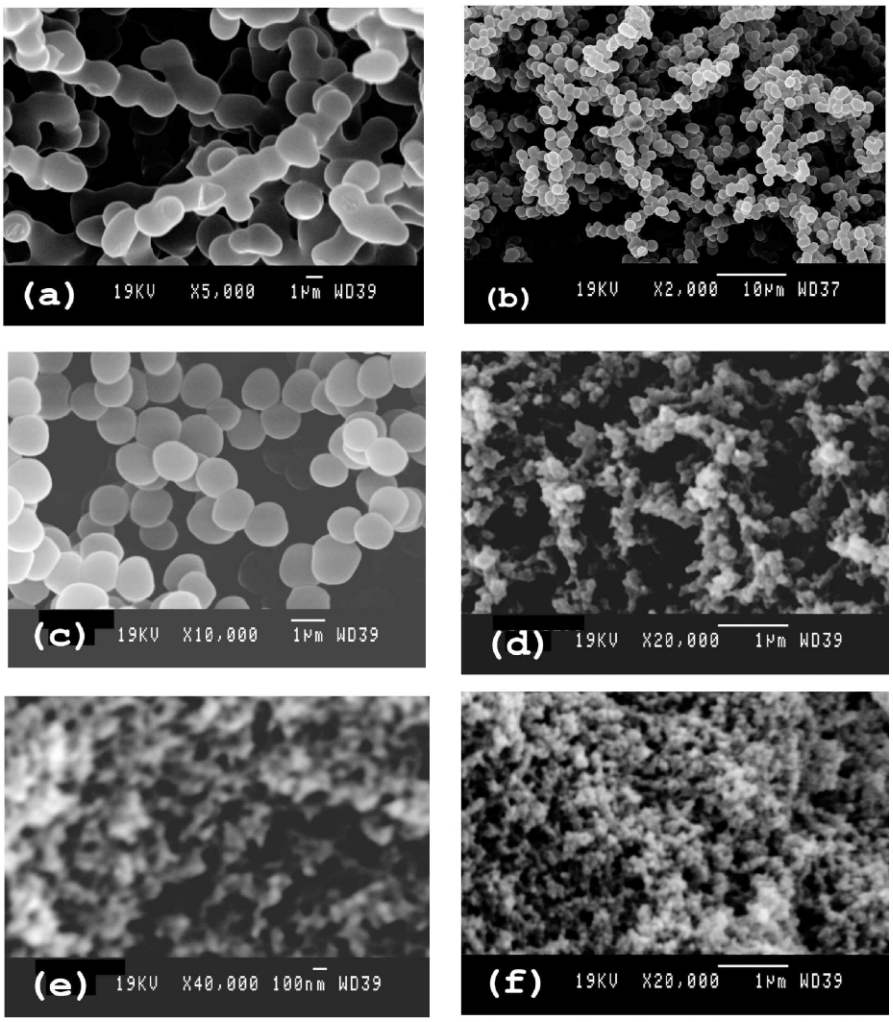

Fig. 5. Particles and aggregates shown on SEM micrographs (a) Sample S1A, (b) Sample S2X, (c) Sample S3X, (d) Sample S4A, (e) Sample S5A and (f) Sample S6A.

chain-like aggregates is characteristic of materials referenced as hyperporous. The usual method for analyzing mercury porosimetry data assumes that mercury intrudes the pore network, and is not appropriate in the present case. A new method was developed to analyze the data of hyperporous materials using Eq. (2), which is based on a model of buckling of the chain-like aggregates. This method is well adapted to the characterization of the polyurethane-based dried gels. Pictures taken on SEM qualitatively confirm the pore size distribution obtained according to this method. It is advisable to be cautious in extrapolating this method to other organic porous materials. The porosity of materials synthesized from a gel is largely open on the external surface, unlike foam synthesized by gas expansion in a polymer in which pores are closed. To our knowledge, no studies have been performed on the crushing of foam constituted by closed cells in the mercury porosimetry experiment, and the relationship between pressure and pore size remains unknown in this latter case.

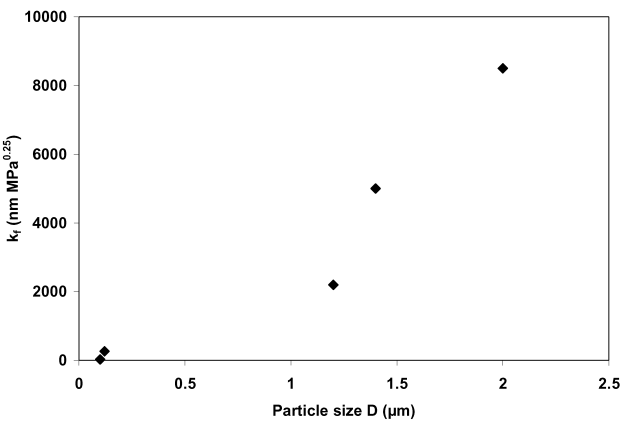

Fig. 6. Correlation between buckling strength k_f and particle size D for the studied polyurethane-based gels.

SEM allows measuring particle size and mercury porosimetry gives an accurate pore size distribution of polyurethane-based aerogels and xerogels. These materials present a significant variation of structural parameters in relation to the synthesis operating variables.

These structural characterizations may permit to better understand the synthesis step followed, and consequently to improve the elaboration process in order to produce efficient insulating materials through a simple process.

Acknowledgements

The authors are grateful to the ADEME (Agence de l'Environnement et de la Maîtrise de l'Energie) for financial support. They are also indebted to the Belgian Fonds National de la Recherche Scientifique, to the Ministère de la Région Wallonne—Direction générale des Technologies et de la Recherche and the Ministère de la Communauté française—Direction de la Recherche scientifique—(action de recherche concertée 00/05-265) for financial support.

References

[1] Washburn EW. Proc Nat Acad Sci 1921;7:115.
[2] Broecker FJ, Heckmans W, Fischer F, Mielke M, Schroeder J, Stange A. In: Fricke J, editor. Proceedings of the First International Symposium on Aerogels, Würzburg, Germany; September 23–25; 1985. Broecker FJ, Heckmans W, Fischer F, Mielke M, Schroeder J, Stange A. In: Fricke J, editor. Proceedings in Physics, Vol. 6. Berlin: Springer; 1986. p. 160–6.
[3] Brinker CJ, Scherer GW. Sol gel science: the physics and chemistry of the sol–gel processing. San Diego: Academic Press; 1990.
[4] Pirard R, Blacher S, Brouers F, Pirard JP. J Mater Res 1995;10:2114.
[5] Alié C, Pirard R, Lecloux AJ, Pirard JP. J Non-Cryst Solids 1999;246: 216.
[6] Pirard R, Pirard JP. In: Unger KK, Kreysa G, Baselt JP, editors. Characterization of porous Solids V. Amsterdam: Elsevier; 2000. p. 603–11.
[7] Smith DM, Johnston GP, Hurd AJ. J Colloid Interf Sci 1990;135:227.
[8] Pirard R, Sahouli B, Blacher S, et Brouers F. J Colloid Interf Sci 1999; 217:216.
[9] Pirard R. Etude de la texture des matériaux hyperporeux par porosimétrie au mercure. PhD Thesis. Université de Liège, ISSN 0075-9333, Liège, Belgium; 2000.
[10] Alié C, Benhaddou A, Pirard R, Lecloux AJ, Pirard JP. J Non-Cryst Solids 2000;270:77.
[11] Biesmans G, Randall D, Français E, Perrut M. J Non-Cryst Solids 1998;225:36.
[12] Biesmans G, Mertens A, Duffours L, Woignier T, Phalippou J. J Non-Cryst Solids 1998;225:64.
[13] Rigacci A, Achard P, Ehrburger-Dolle F, Pirard R. J Non-Cryst Solids 1998;225:260.
[14] Rigacci A, Maréchal JC, Pirard R, Repoux M, Ilbizian P, Chevalier B, Achard P. Proceedings of seventh Meeting on Supercritical Fluids, Antibes-Juan-les-Pins, France; December 6–8; 2000.
[15] Van Bommel MJ, de Haan AB. J Non-Cryst Solids 1995;186:78.
[16] Woignier T, Scherer GW, Alaoui A. J Sol–gel Sci Technol 1994;3: 141.
[17] Alié C, Pirard R, Pirard JP. J Non-Cryst Solids 2001;292:138.
[18] Pirard R, Heinrichs B, Van Cantfort O, Pirard JP. J Sol–gel Sci Technol 1998;13:335.